THE INFLUENCE OF NANOSCALE TOPOGRAPHICAL CUES ON INITIAL OSTEOBLAST MORPHOLOGY AND MIGRATION

E. Lamers[1†], R. van Horssen[2†], J. te Riet[3,4], F.C.M.J.M. van Delft[5], R. Luttge[6], X.F. Walboomers[1], and J.A. Jansen[1*]

[1] Dept. of Biomaterials, Radboud University Nijmegen Medical Centre, Nijmegen, the Netherlands
[2] Dept. of Cell Biology, Nijmegen Centre for Molecular Life Sciences, Radboud University Nijmegen Medical Centre, Nijmegen, the Netherlands
[3] Dept. of Scanning Probe Microscopy, Institute for Molecules and Materials, Radboud University, Nijmegen, the Netherlands
[4] Dept. of Tumor Immunology, Nijmegen Centre for Molecular Life Sciences, Radboud University Nijmegen Medical Centre, Nijmegen, the Netherlands
[5] Philips Research (MiPlaza), Eindhoven, the Netherlands
[6] MESA+ Institute for Nanotechnology, University of Twente, Enschede, the Netherlands

Abstract

The natural environment of a living cell is not only organized on a micrometer, but also on a nanometer scale. Mimicking such a nanoscale topography in implantable biomaterials is critical to guide cellular behavior. Also, a correct positioning of cells on biomaterials is supposed to be very important for promoting wound healing and tissue regeneration. The exact mechanism by which nanotextures can control cellular behavior are thus far not well understood and it is thus far unknown how cells recognize and respond to certain surface patterns, whereas a directed response appears to be absent on other pattern types. Focal adhesions (FAs) are known to be involved in the process of specific pattern recognition and subsequent response by cells. In this study, we used a high throughput screening "Biochip" containing 40 different nanopatterns to evaluate the influence of several nanotopographical cues like depth, width, (an)isotropy and spacing (ridge-groove ratio) on osteoblast behavior. Microscopical analysis and time lapse imaging revealed that an isotropic topography did not alter cell morphology, but it highly induced cell motility. Cells cultured on anisotropic topographies on the other hand, were highly elongated and aligned. Time-lapse imaging revealed that cell motility is highly dependent on the ridge-groove ratio of anisotropic patterns. The highest motility was observed on grooves with a ratio of 1:3, whereas the lowest motility was observed on ratios of 1:1 and 3:1. FA measurements demonstrated that FA-length decreased with increasing motility. From the study it can be concluded that osteoblast behavior is tightly controlled by nanometer surface features.

Key words: Tissue-material interactions, time-lapse imaging, osteoblasts, cell motility, cell adhesion, nanotopography, surface texturing.

*Address for correspondence:
John A. Jansen,
Department of Biomaterials,
Radboud University Nijmegen Medical Centre 309 PB,
PO Box 9101, 6500HB Nijmegen, The Netherlands
Telephone Number: +31 24 3614920
FAX NUmber: +31 24 3614657
E-mail: j.jansen@dent.umcn.nl

† These authors contributed equally to this work

Introduction

In the development of new implantable biomedical materials, several important surface characteristics are currently widely studied, including coating with biochemical signaling molecules (Geiger *et al.*, 2009), wettability (Michiardi *et al.*, 2007), composition (Stone *et al.*, 2009; Rosales-Leal *et al.*, 2010), stiffness (Engler *et al.*, 2006) and topography (Curtis *et al.*, 2001; Walboomers and Jansen, 2001). The latter, surface topography of implantable biomaterials is especially critical to guide cellular behavior like adhesion, spreading and cell movement. In this context (directional) migration and correct positioning of cells on biomaterials are regarded as being very important for promoting wound healing and tissue regeneration. In order to achieve control over these phenomena, previous research has focused on the behavior of cells on substrates provided with organized micron scale topographies, which demonstrated that cellular morphology and migration behavior could be governed by such cues (Su *et al.*, 2007; Kim *et al.*, 2009; Jeon *et al.*, 2010). However, the direct natural environment of a living cell is not (only) organized at the micrometer level, but mainly at the nanometric scale. For example, bone tissue contains an organized array of collagen type-I fibrils with interfibrillar spacings of 68 nm and 35 nm depth (Weiner and Wagner, 1998).

Mimicking nanometric biological surface characteristics in a biomaterial surface is a powerful tool to study and manipulate cellular responses. Dalby *et al.* and Biggs *et al.* studied nanopits and demonstrated that cellular adhesion and spreading decreased, whereas differentiation towards an osteoblastic cell phenotype was promoted (Biggs *et al.*, 2007; Biggs *et al.*, 2008; Dalby *et al.*, 2008). In addition to nanopits, several studies demonstrated that nanometric groove-like structures controlled cellular morphology by inducing alignment to grooves (Clark *et al.*, 1991; Lamers *et al.*, 2010; Loesberg *et al.*, 2007; Tsai *et al.*, 2009; Zhu *et al.*, 2004). Moreover, cell differentiation characteristics can actively be induced by surface nanotopography (Dalby *et al.*, 2007). Although several authors have already studied nanoscale surface features, these were usually spaced in microscale inter distances (Wójciak-Stothard, 1996; Teixeira *et al.*, 2003).

Thus the exact mechanisms by which nanotextures can control cellular behavior are thus far not well understood. In addition, it is unknown how cells are able to recognize and respond to certain surface patterns, whereas a directed response appears to be absent on other pattern types. Still it is generally accepted that focal adhesions (FAs), protein complexes linking the extracellular matrix environment to the intracellular actin cytoskeleton, and adhesive proteins (e.g. integrins) are involved in the process of pattern recognition (Bershadsky *et al.*, 2006).

Immediately after contact of a substrate with cell culture medium, proteins (most importantly fibronectin and vitronectin in serum) start to adhere to the surface (Steele *et al.*, 1992; Garcia and Boettiger, 1999). Specific binding sites in these proteins (the best known being the RGD peptide sequence) are recognized by integrin heterodimers on the cell membrane. The integrins then are assembled in FA complexes of 2-10 μm long and 0.5-1 μm width and are coupled to filamentous (F)-actin by means of linker proteins (e.g., vinculin, paxillin) (Anselme, 2000; Hynes, 2002; Owen *et al.*, 2005; Bershadsky *et al.*, 2006; ; Zaidel-Bar *et al.*, 2007). FAs are formed during initial cell adhesion and thereafter constantly assembled and disassembled during cell movement (Wozniak *et al.*, 2004). In addition, FAs serve as mechanosensors recognizing both biochemical and biophysical characteristics, like surface topography and ligand spacing (Weiss, 1945; Geiger *et al.*, 2009). Maturation of FAs is essential for the establishment of a firm adhesion to a surface and the maintenance of an optimal distance of around 70 nm between activated integrin couples is crucial to induce their clustering (Arnold *et al.*, 2004; Cavalcanti-Adam *et al.*, 2007; Geiger *et al.*, 2009). Upon maturation of FA-complexes, signals are transduced by outside-in and inside-out signaling. Regulation of signaling pathways leads to the control of transcription factors. These transcription factors can, depending on other extracellular signals, activate a cascade of cellular processes, like proliferation, differentiation but also apoptosis (Juliano *et al.*, 2004).

A better understanding of how cells and FAs are affected by specific surface topographical characteristics can support the design and optimization of biomaterials. We hypothesized that individual surface parameters can control osteoblast behavior differently; osteoblast morphology is controlled by pattern shape and dimensions, whereas motility is controlled by pattern spacing and FA organization. In the current study a polystyrene (PS) "Biochip" was used, containing 40 different fields consisting of nanometric surface patterns in order to gain more knowledge on the role of specific nanoscale topographical features on osteoblast morphological behavior (van Delft *et al.*, 2000; Loesberg *et al.*, 2007; van Delft *et al.*, 2008). Each field occupied an area of 500x500 μm^2. Initial osteoblast adhesion, morphology and motility were analyzed in relation to the role of individual surface parameters, i.e., pattern depth and width (a range of pattern dimensions on either deep or shallow substrates), shape (i.e., (an)isotropy) and pattern spacing (three different ridge-to-grooves ratios, i.e., 1:3, 1:1 and 3:1) using this biochip.

Materials and Methods

Substrates

A silicon template containing 40 different nanometric patterns was generated using electron beam lithography (EBL) employing Hydrogen Silsesquioxane resist, as described by Van Delft *et al.* (2000; 2008). The field patterns consisted of 500 x 500 μm^2 areas, containing squares and line patterns with ridge to groove (R:G) ratios of 1:1, 1:3 and 3:1 (Table 1). For obtaining an increased pattern depth, the shallow EBL substrates (non-RIE in Table 1) were used as a mask for standard reactive ion etching (RIE in Table 1). The templates were used to produce polystyrene (PS; Acros, Geel, Belgium) biochips for cell culture (Walboomers *et al.*, 1998).

For the production of the PS replicas, 0.5 g PS was dissolved in 3 mL chloroform and stirred gently overnight. The PS solution was casted onto the silicon wafers and the chloroform was evaporated overnight. The PS substrates were removed from the wafers and 2.0 cm diameter PS rings were glued to substrates using a small amount of casting solution to create cell culture dishes. As a control for cellular orientation smooth substrates were used. All substrates were treated by radiofrequency glow-discharge (RFGD; Harrick Scientific, Pleasantville, NY, USA) for 5 minutes at 10^{-2} mbar for sterilization and to enhance cell adhesion by improving the wettability of the substrate.

Atomic force microscopy (AFM)

After production and sterilization, AFM (Dimension 3100, Veeco, Santa Barbara, CA, USA) with Nanoscope imaging software (version 6.13r1, Veeco) was used to confirm surface topography. Tapping in ambient air was performed with 118 μm long silicon cantilevers (NW-AR5T-NCHR, NanoWorld AG, Wetzlar, Germany) with average nominal

Table 1. Texture dimensions on polystyrene biochip.

Ridge: groove / Pitch (nm)	40	60	80	100	160	200	300	400	600	1000
R:G 1:3		15:45	20:60	25:75	40:120	50:150	75:225	100:300	150:450	
R:G 1:1	20:20	30:30	40:40	50:50	80:80	100:100	150:150	200:200	300:300	500:500
R:G 3:1	30:10	45:15	60:20	75:25	120:40	150:50	225:75	300:100	450:150	750:250
squares		60	80	100	160	200	300	400	600	
RIE*	10.9	11.6	15.3	32.4	51.9	77.4	119.9	149.2	158.0	153.3
Non-RIE**	4.4	7.8	11.0	17.9	30.5	30.6	33.8	34.6	37.3	37.8

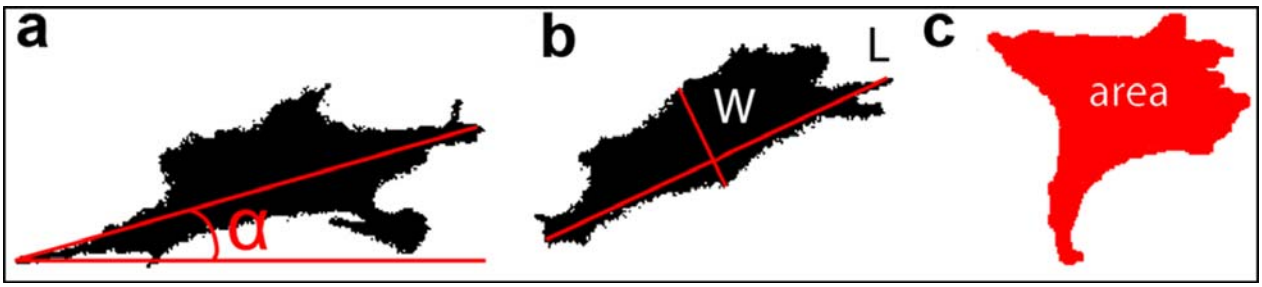

Fig. 1. Overview of methods to measure cellular morphological characteristics. **a.** Orientation was examined by determining the angle (α) between the long cell axis relative to the groove or horizontal square direction. **b.** The elongation factor (EF) was calculated as the length (L) of the long cell axis divided by the maximal length perpendicular to this long axis. **c.** Cell area was measured by creating binary images and measuring the total surface area. All measurements were performed using ImageJ software.

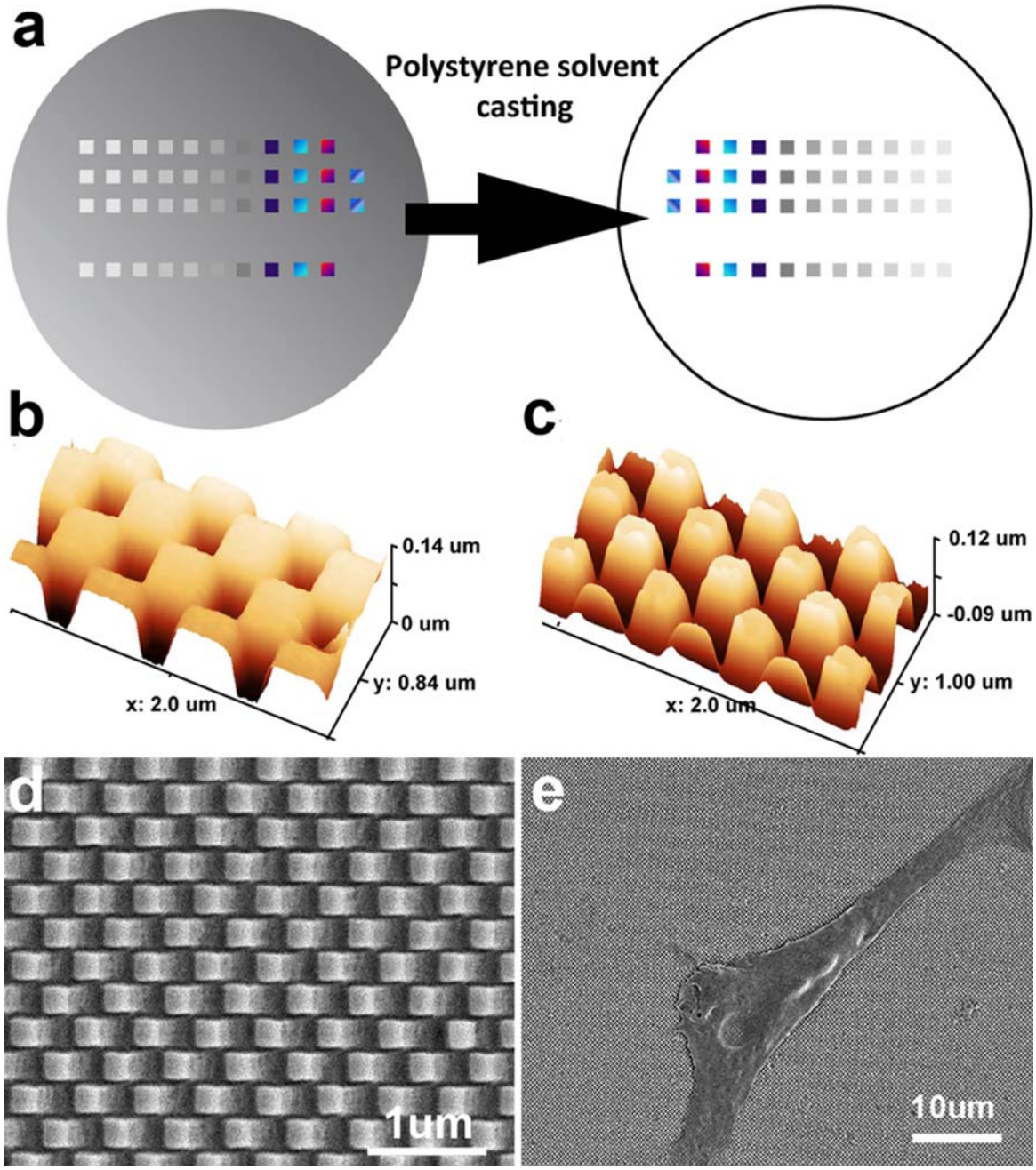

Fig. 2. Polystyrene Biochips are produced from a silicon template and used for biological analyses. **a.** Using polystyrene solvent casting replicas were created containing 40 different field patterns. The **b.** silicon mould and **c, d**. polystyrene replicas were routinely checked with AFM and high resolution SEM. **e.** Polystyrene replicas were finally used for biological analyses.

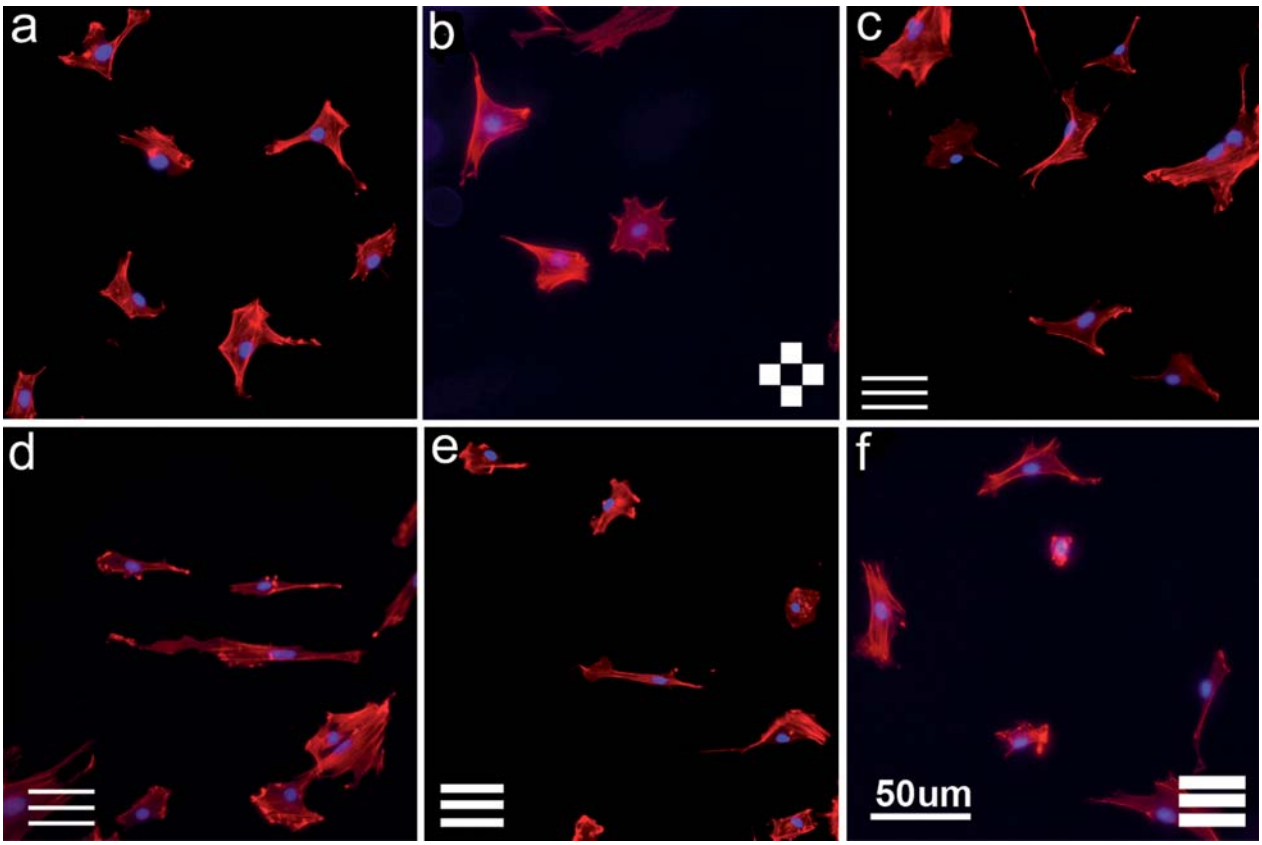

Fig. 3. Osteoblast morphology is influenced by nanogrooves. Stained images of osteoblasts cultured on nanopatterns with a pitch of 200 nm after culturing for 24 hours. Osteoblasts cultured on **a**. smooth control; **b**. nanosquares; **c**. R:G 1:3 and depth of 30.6 nm; **d**. R:G 1:3 and depth of 77.4 nm; **e**. R:G 1:1 and depth of 77.4 nm, and **f**. R:G 3:1 and depth of 77.4 nm. Red: filamentous actin. Blue: nuclei.

resonant frequencies of 317 kHz and average nominal spring constants of 30 N m^{-1}. This type of AFM probe has a high aspect ratio (7:1) portion of the tip with a nominal length of >2 μm and a half-cone angle of <5°. Nominal radius of curvature of the AFM probe tip was less than 10 nm. Height images of each field/sample were captured in ambient air at 50% humidity at a tapping frequency of 266.4 kHz. The analyzed field was scanned at a rate of 0.5 Hz and 512 scanning lines.

Osteoblast-like cell culture

Rat bone marrow (RBM) cells were obtained from femurs of 40-43 day old male Wistar WU rats (local approval #RU-DEC 2008199). The femurs were washed three times in alpha Minimal Essential Medium (aMEM; Gibco, Invitrogen, Paisley, Scotland) with 0.5 mg/mL gentamycin and 3 μg/mL fungizone. The epiphyses were removed and the diaphyses were flushed for RBM isolation with 10 mL osteogenic differentiation medium containing αMEM with 10% fetal calf serum (Gibco), 50 μg/mL ascorbic acid (Sigma-Aldrich, Zwijndrecht, the Netherlands), 10 mM Na-β-glycerophosphate (Sigma), 10^{-8} M dexametasone (Sigma) and 50 μg/ mL gentamycin (Gibco).

RBM cells of two femurs were incubated in differentiation medium in three 75 cm^2 culture flasks (Greiner BioOne, Alphen aan de Rijn, the Netherlands), in a humidified atmosphere of 95% air and 5% CO_2 at 37°C. After one day medium was refreshed to remove non-adherent cells. After 7 days of primary culture, cells were detached with trypsin/EDTA (0.25% w/v trypsin / 0.02 mM EDTA). The cells were concentrated by centrifugation at 1500 rpm for 5 min and resuspended in 10 ml medium. The total cell number was determined with a Coulter® Counter (Coulter Electronics, Luton, UK) and 10^4 cells/ cm^2 were seeded onto the substrates.

Immunofluorescence and quantitative cell measurements

Osteoblasts were cultured for 4 and 24 h, washed in PBS, fixed for 10 minutes in 3% paraformaldehyde (PFA; Fluka, Sigma-Aldrich and 0.02% glutaraldehyde (Acros) in phosphate buffered saline (PBS), permeabilized in 1% Triton X100 (Koch, Colebrook, UK) in PBS for 5 minutes and incubated with PBS containing 5% bovine serum albumin (BSA) (Sigma) for 30 minutes to block aspecific epitopes. Vinculin staining was performed overnight with mouse monoclonal primary antibodies (1:1000; Sigma) in PBS containing 1% BSA and 0.1% Tween-20, followed by goat anti-mouse secondary antibody Alexa-fluor 488 conjugated IgG (1:200; Molecular Probes, Invitrogen), Alexa-fluor 568 conjugated phalloidin for filamentous actin fluorescence (1:200; Molecular Probes, Invitrogen) and DAPI (4',6-diamidino-2-phenylindole) staining for nucleic ultra-violet (UV)-visualization (1:2500) diluted in PBS containing 1% BSA and 0.1% Tween-20 (Merck, Schuchardt, Germany) for 2 hours at room temperature.

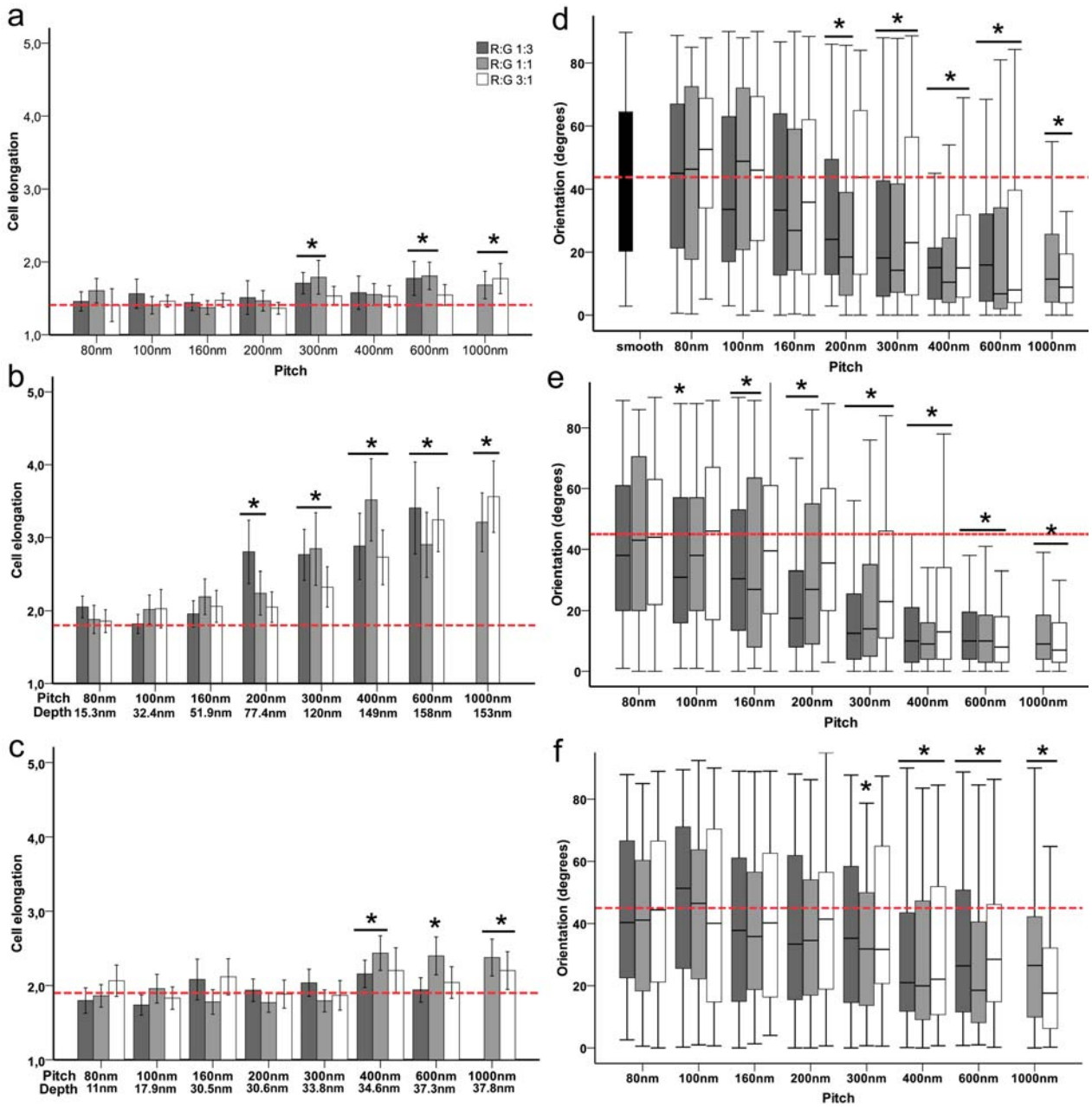

Fig. 4. Osteoblast elongation and orientation are dependent on groove width and depth. Cell elongation was measured after **a**. 4 hours on deep substrates, **b**. 24 hours on deep substrates and **c**. 24 hours on shallow substrates. The red line indicates the mean elongation of cells on a smooth control. Error bar represents 95% confidence interval. * $P<0.05$ relative to smooth control. A Box-Whisker plot showing osteoblast alignment to nanogrooves. The median is marked in the box and the box-corners indicate the 25th to 75th percentiles; whiskers indicate the 5th and 95th percentile. Orientation was measured after **d**. 4 hours on deep substrates, **e**. 24 hours on deep substrates, and **f**. 24 hours on shallow substrates. The red line indicates the median orientation of cells on a smooth control. * $P<0.05$ relative to smooth control.

Samples were examined using an Olympus FV1000 confocal laser scanning microscope with a 40x water immersion objective (CLSM, Olympus, Center Valley, PA, USA).

Orientation of osteoblasts on nanopatterns was examined by analyzing over 100 cells per substrate and determining their angle relative to the groove or horizontal square direction. The elongation factor (EF) was defined as the length of the longest cell axis divided by the maximal length perpendicular to this long axis. The cell area was measured by creating binary images and measuring the total surface area (Fig. 2). Analysis of FA was performed by measuring 20 cells per substrate and determining length of all FA present. All measurements were performed using ImageJ software (Image J, National Institutes of Health, Bethesda, MD, USA). Statistical analysis was performed by performing either an unpaired *t*-test (elongation and FA-length) or a non-parametric Wilcoxon signed rank test (orientation and area). Statistical analysis was performed using SPSS for Windows (SPSS14.0, Chicago, IL, USA).

Time-lapse imaging

Time-lapse imaging of migrating cells was performed for 24 h in a Microscope Stage Incubator (Oko-Lab, Quarto (NA), Italy), ensuring optimal culture conditions, using a Nikon (Tokyo, Japan) DiaPhot microscope equipped with a Hamamatsu (Hamamatsu City, Japan) C8484-05G digital camera. Cells were cultured on the RIE-biochips and imaged with a 10x objective every 10 minutes using TimeLapse Software (Oko-Lab), version 2.7. From the resulting time-lapse movies, cell motility was analyzed by tracking the migration paths of individual cells, taking the nuclei as a reference. For each nanopattern dimension at least 35 cells were tracked. After cell division one daughter cell was followed. The motility (total migrated track distance; T) and the straight displacement (D, distance from start to end point) were measured. Directionality of cell movements was measured as the D/T ratio. Measurements were performed using ImageJ software with the MTrackJ plugin.

Results

Nanopatterned substrates

Both RFGD treated polystyrene biochips (RIE and non-RIE) containing 40 different fields of nanopatterns consisting of squares, and grooves with different spacings (Table 1) were routinely checked on the quality of replication by means of AFM and SEM (Fig. 2). Nanopatterns with a pitch smaller than 80 nm (i.e. the sum of groove and ridge width) appeared to be too small for an accurate replication process and were therefore excluded from further analysis.

Osteoblast elongation

After 4 hours of culture on the smooth control, osteoblasts were only marginally elongated (Elongation Factor, EF =

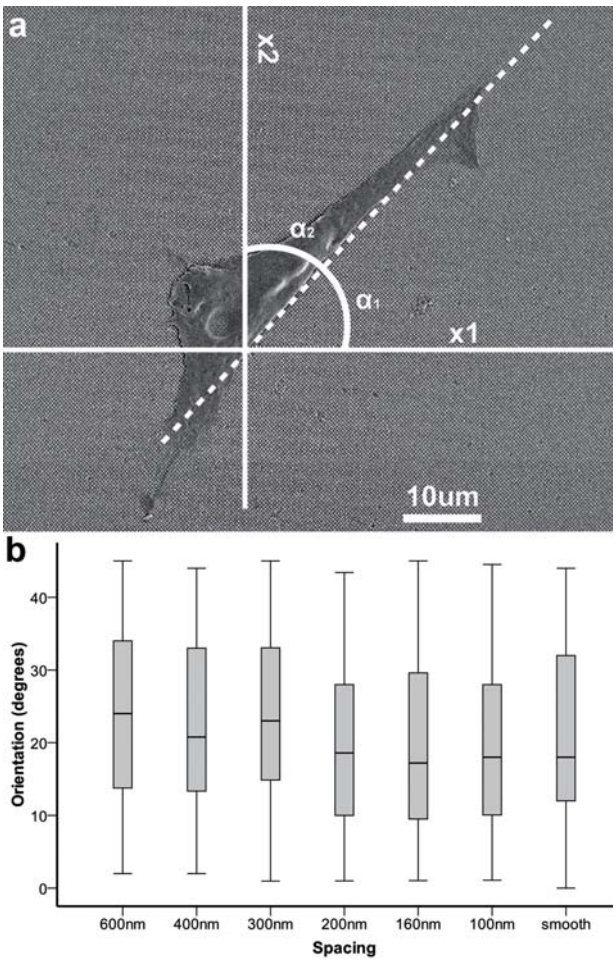

Fig. 5. Osteoblasts orient randomly on nanosquares. Osteoblast orientation on nanosquares was measured. Due to the isotropy, osteoblasts can orient parallel to the pattern in two directions (x1 and x2). Therefore, orientation of osteoblasts was measured as the shortest angle from one of two axes and maximal orientation angle was 45°.

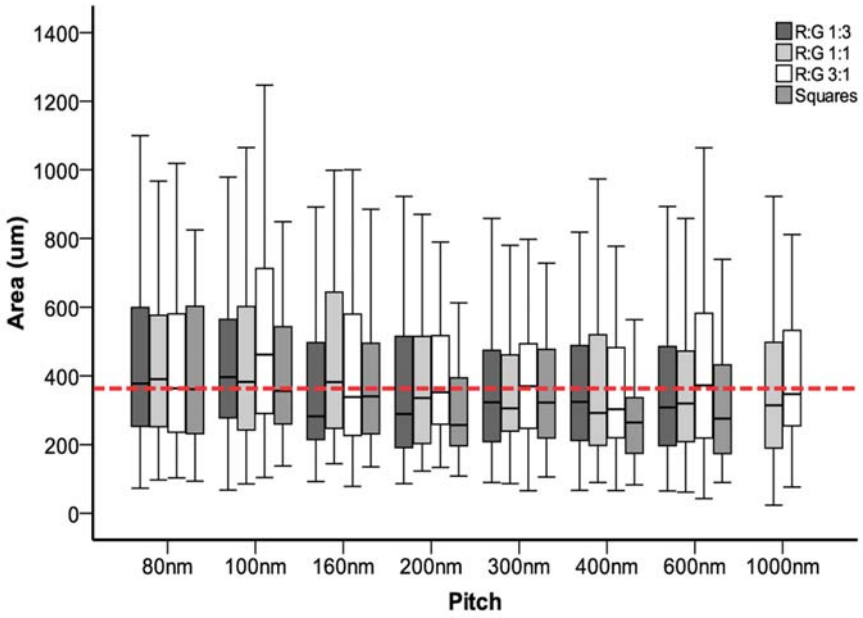

Fig. 6. Nanopatterns do not affect osteoblast cell area. Average osteoblast area on high nanopatterns after 24 hours of culture. Red line: median area of osteoblasts cultured on smooth substrates. No significant differences were observed between the various substrates.

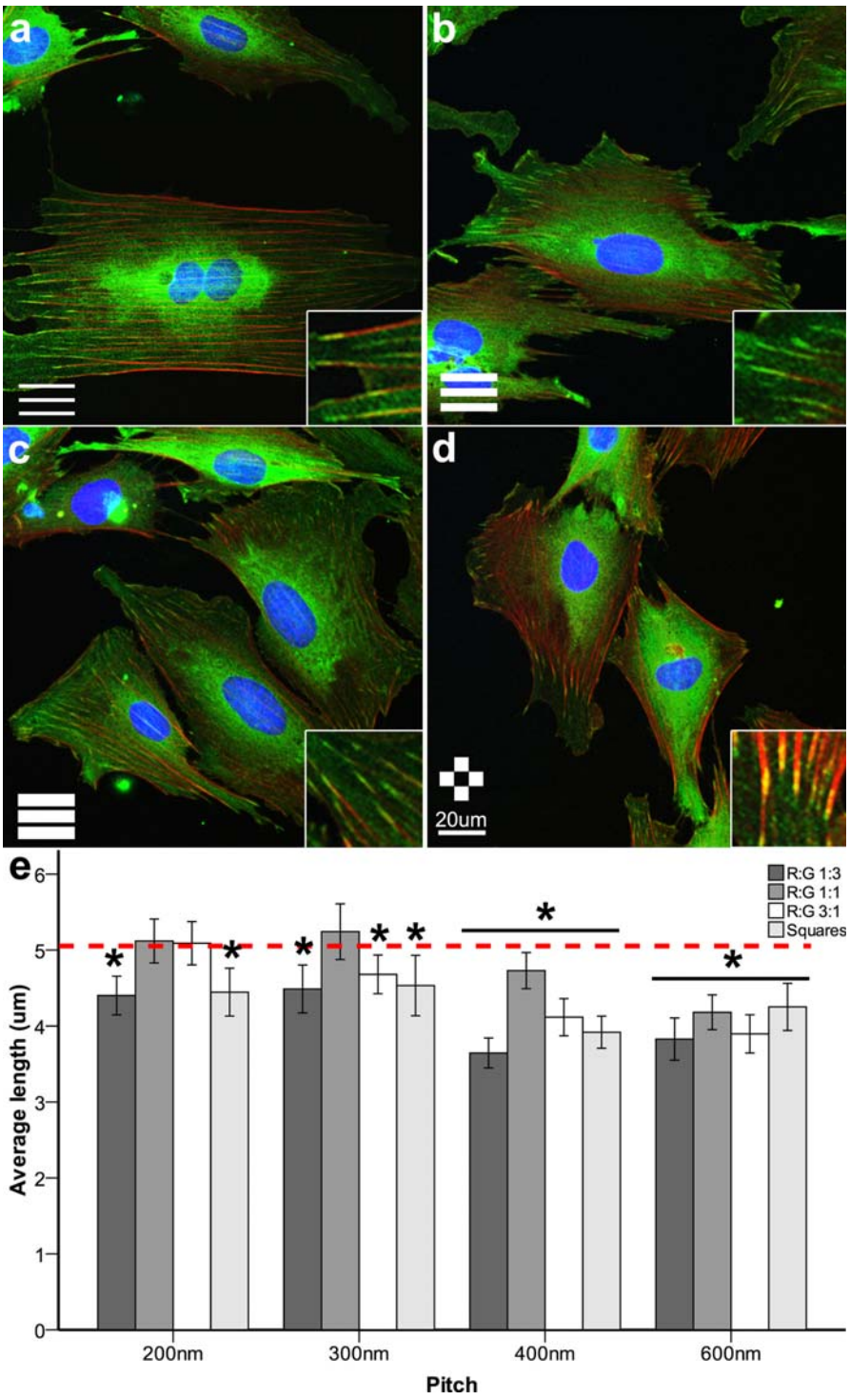

Fig. 7. Focal adhesion length is influenced by nanopatterns. Immunofluorescence stainings of osteoblasts cultured on nanopatterned substrates with a 300 nm pitch. **a**. R:G of 1:3; **b**. R:G of 1:1; **c**. R:G of 3:1 and **d**. squares. Green: vinculin; red: F-actin; blue: nuclei. Bar: 20 μm. Inset are magnified images of focal adhesions. **e**. FA-length was measured after 24 hours. Red line indicates the mean FA length on a smooth control. * $P<0.05$ relative to smooth control.

1.4±0.11). After 24 hours of culture on smooth substrates, cells had spread more and were significantly more elongated (EF = 1.9±0.17, $P<0.05$).

Staining of osteoblasts cultured on isotropic nanosquares revealed that morphology was similarly influenced as osteoblasts cultured on the smooth control; cells did not appear to be elongated in a specific direction (Fig. 3). Elongation measurements confirmed these observations, as the EF was similar to the smooth control up to 400 nm spacing. On a spacing of 600 nm cells were significantly more elongated (EF = 2.2±0.25; $P<0.05$; data not shown).

Depending on the pitch (i.e., sum of groove and ridge width), osteoblasts cultured on anisotropic nanogrooved substrates were clearly more elongated than on the smooth substrate and also were oriented into the groove direction. Measurements demonstrated that osteoblast elongation was dependent on three groove parameters, i.e., spacing, depth

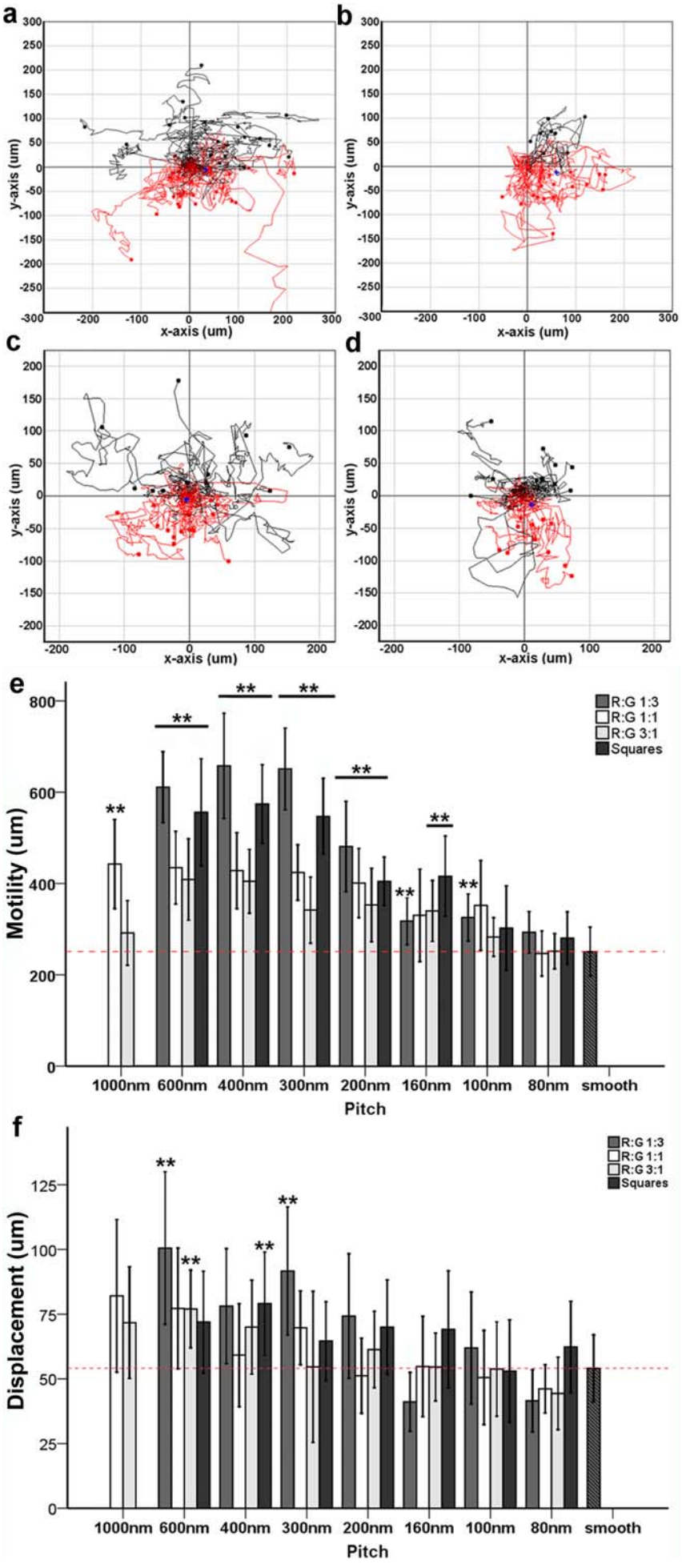

Fig. 8. Osteoblast motility is altered by increasing surface topography and pattern dimensions. Motility plots of osteoblasts cultured for 24 hours on a **a**. R:G of 1:3 and 600 nm pitch; **b**. squares and 600 nm pitch; **c**. R:G 1:3 and 200 nm pitch; **d**. squares and 200 nm pitch. **e**. Total motility of osteoblasts on nanopatterns in 24 hours. **f**. Displacement of osteoblasts on nanopatterns. Error bars represent 95% confidence interval. * $P<0.05$ relative to smooth control. Red line: average motility or displacement of osteoblasts cultured on a smooth control.

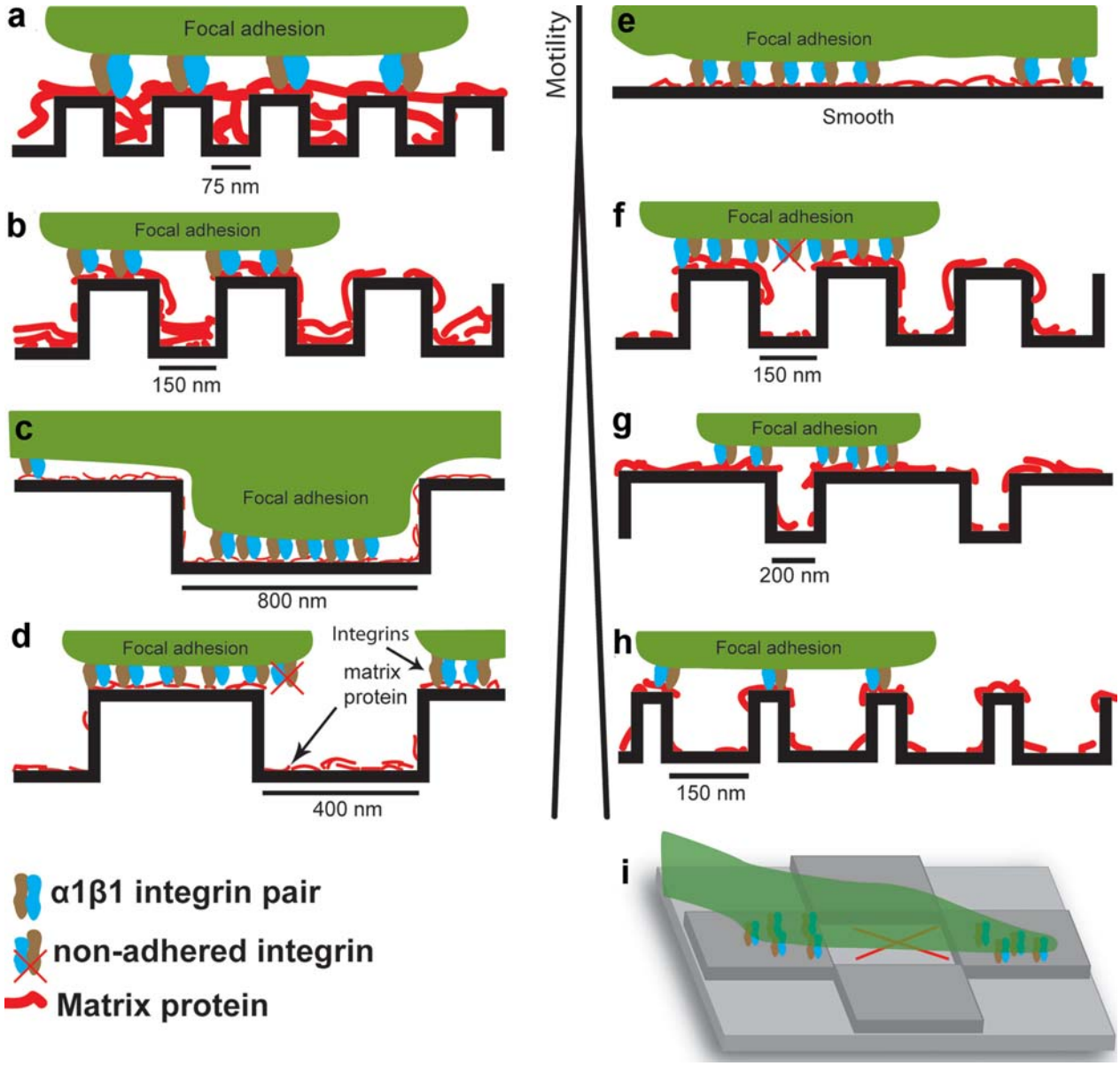

Fig. 9. Hypothesized models to explain the role of focal adhesions and matrix proteins in the response of osteoblasts to groove width and ridge-groove ratio. **a**. FAs respond similar to grooves smaller than 75 nm wide as to smooth substrates (**e**); cell adhesion is firm and motility will be low. **b**. FAs on 150 nm wide grooves cross several ridges by which adhesive strength will decrease and motility will increase. **c**. FAs on grooves wider than 0.5 µm can descend into the grooves and this results, depending on the ridge width, in a firm adhesion and a decreasing motility. **d**. FAs of 0.5µm width reside on top of the ridges and cannot descend into grooves. Depending on the ridge width, motility will be high. **f**. An alternatively proposed model for **b**. The maximal distance between integrins for maturation and normal intracellular signaling is ≤75 nm. If the distances become greater (or if integrins cannot reach a target) signaling is impaired and cellular response will change. This results in an increased motility of the cells. **g**. On a high R:G, more integrins per FA can adhere to the substrate and this results in an increased adhesion strength and decreased motility. **h**. On a low R:G FA response will be severely decreased and this results in a high motility. **i**. On squares, cell motility is high due to the inability to form mature FA over the complete FA length.

and width. At 4 hours, osteoblast elongation on a R:G of 1:3 and 1:1 was significantly increased on grooves down to a pitch of 300 nm (EF = 1.7±0.15 and 1.8±0.2 respectively), whereas on a R:G of 3:1 only a significantly increased response was observed down to a pitch of 1000 nm (EF = 1.5±0.1; Fig. 4a). At 24 hours, a similar trend was observed, as osteoblasts were most responsive to grooves with a R:G of 1:3 and 1:1 and cells were less responsive to a R:G of 3:1. Maximal elongation was observed for cells cultured on a pattern with a R:G of 1:1 and 400 nm pitch (EF = 3.5±0.6).

A sufficient pattern depth appeared to be an important factor for osteoblast elongation (Fig. 4b,c). Cells were significantly elongated on grooves down to a minimal pitch of 200 nm when the depth was >77.4 nm. When pattern depth was reduced, osteoblasts significantly elongated down to a minimal pitch of 400 nm, with a depth of 34.6 nm albeit to a lesser extent.

Table 2. Directionality (displacement/total movement) and migration velocity of osteoblasts.

Smooth	**0 nm**							
Directionality (D/T)	0.22							
Migration velocity (μm/min)	0.17 ±0.04							
R:G 1:3		**600 nm**	**400 nm**	**300 nm**	**200 nm**	**160 nm**	**100 nm**	**80 nm**
Directionality (D/T)		0.16	0.12	0.14	0.15	0.13	0.19	0.14
Migration velocity (μm/min)		**0.42 ±0.05**	**0.46 ±0.08**	**0.45 ±0.06**	**0.33 ±0.07**	0.22 ±0.03	**0.23 ±0.04**	0.20 ±0.03
R:G *1:1*	**1000 nm**	**600 nm**	**400 nm**	**300 nm**	**200 nm**	**160 nm**	**100 nm**	**80 nm**
Directionality (D/T)	0.19	0.18	0.14	0.16	0.13	0.17	0.14	0.19
Migration velocity (μm/min)	**0.31 ±0.07**	**0.30 ±0.05**	**0.30 ±0.06**	**0.29 ±0.04**	**0.28 ±0.05**	0.23 ±0.07	0.24 ±0.07	0.17 ±0.03
R:G 3:1	**1000 nm**	**600 nm**	**400 nm**	**300 nm**	**200 nm**	**160 nm**	**100 nm**	**80 nm**
Directionality (D/T)	0.25	0.19	0.17	0.16	0.17	0.16	0.19	0.18
Migration velocity (μm/min)	0.20 ±0.05	**0.28±0.06**	**0.28 ±0.05**	**0.24 ±0.05**	**0.25 ±0.05**	**0.24 ±0.05**	0.20 ±0.03	0.17 ±0.03
Squares		**600 nm**	**400 nm**	**300 nm**	**200 nm**	**160 nm**	**100 nm**	**80 nm**
Directionality (D/T)		0.13	0.14	0.12	0.17	0.17	0.18	0.22
Migration velocity (μm/min)		**0.39 ±0.08**	**0.40 ±0.06**	**0.38 ±0.06**	**0.28 ±0.04**	**0.29 ±0.06**	0.21 ±0.06	0.19 ±0.04

The different response of osteoblasts to pattern spacing could be explained by the groove width (Fig. 4b). Osteoblasts cultured on grooves with a R:G of 3:1 were significantly elongated down to a minimal groove width of 75 nm (225 nm ridge width; EF = 2.3±0.3), on a R:G of 1:1 osteoblasts were elongated down to 100 nm groove width (100 nm ridge width; EF = 2.2±0.2) and on a R:G of 1:3 cells were elongated down to a groove width of 125 nm (75 nm ridge width; EF = 2.8±0.4).

Osteoblast orientation

Since the data from the analysis by definition are skewed a box-whisker plot was drawn which shows the median (line in the box), 1st and 3rd quartiles (box edges) and the 5th and 95th percentile (whiskers). Osteoblasts cultured on smooth substrates displayed a random orientation (median of ~45°; Fig. 4), independent of culture time.

As nanosquares are isotropic, and thus have two horizontal axes, osteoblasts can orient only at a maximum angle of 45° relative to one of both horizontal axes (Fig. 5). Hence osteoblast orientation was measured relative to the shortest axis, which always had a maximum of 45°. Use of this different measuring approach demonstrated that osteoblasts were randomly orientated on the nanosquares with median orientations between 20 and 30°.

In contrast, a highly aligned morphology of osteoblasts was induced by nanogrooves. The analysis demonstrated that alignment was even more dependent on the surface topographical parameters (spacing, pattern depth and width) than elongation. At 4 hours, osteoblasts were most responsive to a R:G of 1:3 and 1:1 and significantly aligned to a groove pitch down to 200 nm relative to the smooth substrates, whereas on a R:G of 3:1 osteoblasts aligned to a pitch down to 300 nm (Wilcoxon signed rank test $P<0.05$, Fig. 4d). The importance of the R:G became even more evident at 24 hours. Osteoblasts cultured on a R:G of 1:3 displayed the highest sensitivity, and significantly aligned to a pitch down to 100 nm. Cells cultured on a R:G of 1:1 were responsive to a minimal pitch of 160 nm. Osteoblasts were least responsive to a R:G of 3:1; cells aligned down to a pitch of 300 nm (Fig. 4e). The differences in sensitivity to pattern spacings are a result of the groove width. On all three R:G ratio's, cells aligned to a minimal groove width of 75 nm, irrespective of ridge width, indicating that this dimension is a clear threshold for specific pattern recognition.

The importance of pattern depth was more pronounced on osteoblast alignment than on elongation as demonstrated by the graphs in Fig. 4e and f. Osteoblasts cultured on the non-reactive ion etched (RIE) patterns with decreased depth were most responsive to a R:G of 1:1 (Fig. 4f). Cells aligned to a pitch of 300 nm with a width of 33.8 nm. Osteoblasts were less responsive to a R:G of 1:3 and 3:1; cells aligned to a groove width down to 400 nm with a depth of 34.6 nm. Surprisingly however, osteoblasts cultured on the RIE biochip and a R:G of 1:3 did align to a pitch of 100 nm with a depth of 32.4 nm (Fig. 4e).

Osteoblast area

On smooth substrates, the median osteoblast area was 391 μm (Fig. 6). Osteoblast area appeared not to be decreased by the squares nor nanogrooves on all tested R:G ratios, pitches and depths, indicating that elongation effects are not explained by an overall increase in cell spreading.

Focal adhesions

To determine the influence of nanopattern dimensions on osteoblast adhesion in more detail, FAs were analyzed (after 24 hours of culture only) on the nanopatterned RIE biochip (Fig. 7). On the smooth control, cells displayed an average FA length of 5.1±0.3 μm. Osteoblasts cultured on the nanopatterns demonstrated that an increase of the pattern size resulted in a significantly decreased FA length (*t*-test, $P<0.05$). The smallest FAs were observed on

patterns with a R:G of 1:3; FAs on all studied pitches were significantly smaller than on the smooth control. Cells cultured on a R:G of 1:1 displayed the longest FAs; a significant difference with the smooth control was observed from a minimal groove pitch of 400 nm. The influence of nanopatterns on the amount of FAs in each cell was also determined, but there were no differences (data not shown).

Osteoblast motility

For measurements of motility (T), displacement (D) and directionality (i.e., D/T), motility plots were created (Fig.8 a-d) (Pankov *et al.*, 2005). These motility plots demonstrated that, in contrast to osteoblast alignment on grooves, the orientation of cell movement was random on all studied grooved substrates.

After initial adhesion and spreading on smooth substrates, osteoblast motility (251±51 μm) as well as displacement remained low over 24 hours at an average speed of 0.17±0.04 μm/min (Movie 1 and Table 2). Osteoblast directionality was 0.22 of all cell movements (Fig.8 e,f).

Osteoblast motility was influenced by several topographical factors like pattern shape, pattern spacing and width (Movies 2,3; grooves are in horizontal direction). Whereas osteoblast morphology was barely affected by the isotropic nanosquares, these patterns greatly increased motility; on a pattern spacing of 400 nm the highest motility was observed (574±79 μm). The average motility of osteoblasts on 400 nm spaced nanosquares was significantly increased not only relative to the smooth control ($P<0.05$), but also relative to grooves with a R:G of 1:1 (428±82 μm) and 3:1 (405±69 μm; $P<0.05$). Displacement of cells on the other hand was only marginally increased and this resulted in a decreased directionality compared to the smooth control. Osteoblast motility on nanosquares was increased down to a pattern spacing of 160 nm (415±69). Displacement on this pattern was not significantly increased relative to the smooth control.

In addition to surface isotropy, groove spacing (R:G) and width greatly affected osteoblast motility. Whereas maximum motility was observed on a 400 nm pitch for all three ratios, osteoblasts were significantly more motile on a R:G of 1:3 (658±75 μm) compared to a R:G of 1:1 and 3:1. This phenomenon was persistent down to a pitch of 200 nm (Fig. 8e). Relative to the smooth control, osteoblast motility on a R:G of 1:3 was increased down to a pitch of 100 nm (325±51 μm). The displacement on the other hand remained relatively low and hence cells cultured on a R:G of 1:3 had a lower directionality than cells cultured on smooth control. Osteoblasts cultured on a R:G of 1:1 and 3:1 moved in a similar speed on all studied pitch dimensions. An increased osteoblast motility on a R:G of 1:1 was persistent down to 200 nm pitch, whereas it persisted down to 160 nm on a R:G of 3:1. Displacement and directionality on these groove ratios were decreased relative to the smooth control.

Discussion

In the current study we aimed to get insight in how osteoblast morphology and motility are controlled by nanoscale surface features like (an)isotropy, spacing (R:G) and depth using a biochip with an array of nanoscale squares and groove patterns differing in depth, width, spacing and ridge-groove ratio. By the use of such a biochip, a wide range of specific nanoscale topographical factors on cell behavior can be studied in a high throughput screening method. In order to obtain a large number of biochips, as were needed in the study, polystyrene replicas were created by solvent casting. The patterns on the biochip were highly reproducible into polystyrene down to a pitch of 80 nm as demonstrated by AFM and SEM. As stated by Van Delft *et al.* (2008), most likely the diffusion limitation in the smallest grooves during RIE resulted in shallower depths and more concave grooves. Additionally, the capillary forces of the smallest patterns could also affect reproduction accuracy by PS solvent casting.

The data demonstrate that osteoblast morphology and motility can be specifically controlled by nanoscale surface features, like depth, width, isotropy and spacing. By observation of osteoblasts using fluorescence microscopy, isotropic nanotopography appeared to have only a little influence on the overall osteoblast shape. Detailed SEM observation by Dalby *et al.* (2004a, 2004b) showed that cells on isotropic nanoscale topography still exhibit unique features. Fluorescence microscopical evaluation of anisotropic nanogrooves on the other hand, affected morphology to much greater extent. Although by nature cells in culture are elongated (i.e., EF of 1.5 of cells on a smooth control), when cultured on grooves elongation is increased in conjunction to the alignment. In line with several other studies, depending on groove width, depth and spacing cells became highly elongated and aligned into the groove direction (Teixeira *et al.*, 2003; Yang *et al.*, 2008; Liliensiek *et al.*, 2010). The alignment of cells to grooves is possibly dependent on the tyrosine phosphorylation of actin binding proteins as previously shown by Wójciak-Stothard *et al.* (1996). Still this study confirmed that a threshold for cellular response to anisotropic substrates exists at a 75 nm groove width (Loesberg *et al.*, 2008; Tocce *et al.*, 2010). Moreover, our study demonstrated that this threshold value was irrespective of ridge width. Unmistakably, cells were most responsive to grooves with a R:G of 1:3 over equal or reversed ridge-groove ratios indicating the importance for the sufficient groove width. In addition, pattern depth greatly influenced osteoblast morphology, independent of spacing. In agreement with previous studies, a threshold for the response to pattern depth was found at ~34 nm (Lenhert *et al.*, 2005; Loesberg *et al.*, 2008). The inability to respond to patterns with a depth less than 34 nm may be hypothesized to be a result of clogging of the surface features in a protein rich environment. The adhesion of serum proteins from the medium, like fibronectin and vitronectin, cover the groove surface as well as the ridge surface thereby "smoothening" the substrate by forming a ubiquitously adhesive surface for cells by which the

nanopatterns are no longer recognized by integrins (as illustrated in Fig. 9a) (Toworfe *et al.*, 2004). Although cells upon seeding produce ECM cell adhesion proteins, future studies in serum free media or integrin inhibition studies could be applied to study specific effects on such small patterns in more detail.

In addition to cell morphology, time-lapse imaging analysis was used to analyze cell motility. The results demonstrated that although osteoblast morphology was not affected by isotropic nanosquares, motility was highly increased on such surfaces. Cell motility on grooves was, like morphology, highly dependent on groove width and space. Similar observations were also made by Wójciak-Stothard *et al.* (1995), who demonstrated that macrophage motility was increased by groove depths decreasing to the sub-micrometer range. On grooves with a R:G of 1:3 as well as on the squares, motility was significantly higher compared to grooves with a R:G of 1:1 and 3:1 with a maximum motility at a pitch of 400 nm. A possible explanation for differential cell behavior on various substrate textures might be that the micro-mechanic properties directly at the surface are altered (Engler *et al.*, 2006). However, the polystyrene used in our experiments is a rigid material (Khatiwala *et al.*, 2006). Moreover, structural changes in the cells are recognized on different patterns. Interestingly, FAs possessed the shortest length on both squares and grooves with a R:G of 1:3 and a pitch of 400 nm, suggesting that integrin cluster size, which results in FA binding strength, is decreased (Fig. 9f-i). Coussen *et al.* (2002) demonstrated that groups of only three integrin pairs are needed to form an activated cluster and establish adhesion. An increase of integrin clusters will lead to enlarged FAs, increased FA maturation and adhesion strength. This will consequently lead to a decrease in motility. Previous studies already demonstrated that FA reside on top of the ridges parallel to nanoscale grooves (Fujita *et al.*, 2009; Lamers *et al.*, 2010). From this knowledge, we hypothesize that for the formation of mature, long integrin clusters, which leads to FA maturation and thus cell adhesion on nanopatterns, either sufficient ridge width or groove width is essential.

This hypothesis is confirmed by the results in the current study as well as other studies. First, motility data demonstrated that ridge width determines the rate of motility. The ridge width and thus the ability to form large clusters if the formation of mature FAs on a low R:G is limited (Fig.9h) and therefore cell motility will be higher compared to a high R:G with a greater amount of possible adhesion spots (adhesive area) for integrins (Fig. 9f,g). In addition, cells did not respond to a groove width of <75 nm. This can be either a result of proteins covering the grooves (Fig. 9a), or of the ability of cells to form large integrin clusters by adhering to multiple ridges with a critical distance of <75 nm as shown by the group of Spatz (Arnold *et al.*, 2004; Cavalcanti-Adam *et al.*, 2007; Geiger *et al.*, 2009). In these studies, it was demonstrated that there is a maximal distance between integrin binding sites for integrin clustering (in a range of 50-70 nm) above which cells fail to develop mature FAs resulting from restrained integrin signaling. In this context, adjacent integrin pairs bridge grooves of ≤75 nm width and form clusters without "recognizing" the space between the grooves. On the other hand, integrin signaling on grooves >75 nm is impaired because the space between two adjacent integrins is >75 nm, which results in a decreased integrin clustering, reduced FA maturation and increased motility as observed with time-lapse imaging (Fig. 9b,d) (Cavalcanti-Adam *et al.*, 2007; Shattil *et al.*, 2010). In order to establish adhesion, integrins residing parallel on the ridges form clusters to become activated. Consequently, cells become elongated and align parallel to the grooves (Fujita *et al.*, 2009). On groove widths >500 nm cell motility decreased, although cells remained elongated and aligned parallel to the groove direction. At this point, grooves are wider than the minimal FA width and possibly large integrin clusters can form inside the spaces, but with low efficiency (Fig. 9c). Uttayarat *et al.* (2008) demonstrated that FAs also reside inside grooves of sufficient width. Possibly, the 500 nm groove width as studied by them can be considered as a threshold for FA-sensing inside the grooves as the minimal FA width is approximately 500 nm (Hynes, 2002).

In order to further confirm this hypothesis, additional experiments should be carried out, such as atomic force microscopy analysis to measure the adhesion strength of cells on nanopatterns. FA maturation can be studied by measuring phosphorylation of proteins downstream in the outside-in signaling pathway like FAK or proteins in the mitogen activated protein kinase pathway (MAPK) Hamilton *et al.*, 2007; Kim *et al.*, 2007). FAK is autophosphorylated upon integrin engagement to a target and activation by clustering of integrin pairs (Kirchner *et al.*, 2006). Activation of FAK results in activation of the MAPK pathway, which leads to the activation of transcription factors (Juliano *et al*. 2004).

Conclusion

In the current study, a high throughput "Biochip" was used to evaluate the role of different nanometer features, like (an)isotropy, pattern depth, width and spacing on (initial) cellular behavior by performing analyses on cell morphology, FAs as well as motility. From the study, it can be concluded that nanometer features tightly control osteoblast behavior. Osteoblast morphology is highly controlled by surface anisotropy and motility is specifically controlled by the ridge-to-groove ratio as osteoblasts are most motile on a R:G of 1:3 and a pitch of 400 nm. Isotropic nanosquares do not induce morphological changes on osteoblasts, but they specifically enhance motility up to a maximum at a pattern spacing of 400 nm. The obtained knowledge can aid the further development of smart surfaces that control cell behavior and account for improved osseointegration around orthopedic and dental implants.

Acknowledgments

Time-lapse imaging and confocal laser scanning microscopy were performed at the microscope imaging centre (MIC) of the Nijmegen Centre for Molecular Life Sciences (NCMLS).

This research is supported by the Dutch Technology Foundation STW, applied science division of NWO and the Technology Program of the Ministry of Economic Affairs (project # 07621)

References

Anselme K (2000) Osteoblast adhesion on biomaterials. Biomaterials **21**: 667-681.

Arnold M, Cavalcanti-Adam EA, Glass R, Blummel J, Eck W, Kantlehner M, Kessler H, Spatz JP (2004) Activation of integrin function by nanopatterned adhesive interfaces. Chemphyschem **5**: 383-388.

Bershadsky AD, Ballestrem C, Carramusa L, Zilberman Y, Gilquin B, Khochbin S, Alexandrova AY, Verkhovsky AB, Shemesh T, Kozlov MM (2006) Assembly and mechanosensory function of focal adhesions: Experiments and models. Eur J Cell Biol **85**: 165-173.

Biggs MJ, Richards RG, Gadegaard N, Wilkinson CD, Dalby MJ (2007) The effects of nanoscale pits on primary human osteoblast adhesion formation and cellular spreading. J Mater Sci Mater Med **18**: 399-404.

Biggs MJ, Richards RG, Gadegaard N, McMurray RJ, Affrossman S, Wilkinson CD, Oreffo RO, Dalby MJ (2008) Interactions with nanoscale topography: Adhesion quantification and signal transduction in cells of osteogenic and multipotent lineage. J Biomed Mater Res A **18**: 399-404.

Cavalcanti-Adam EA, Volberg T, Micoulet A, Kessler H, Geiger B, Spatz JP (2007) Cell spreading and focal adhesion dynamics are regulated by spacing of integrin ligands. Biophys J **92**: 2964-2974.

Clark P, Connolly P, Curtis ASG, Dow JAT, Wilkinson CDW (1991) Cell guidance by ultrafine topography *in vitro*. J.Cell Sci **99**: 73-77.

Coussen F, Choquet D, Sheetz MP, Erickson HP (2002) Trimers of the fibronectin cell adhesion domain localize to actin filament bundles and undergo rearward translocation. J Cell Sci **115**: 2581-2590.

Curtis AS, Casey B, Gallagher JO, Pasqui D, Wood MA, Wilkinson CD (2001) Substratum nanotopography and the adhesion of biological cells. Are symmetry or regularity of nanotopography important? Biophys Chem **94**: 275-283.

Dalby MJ, Gadegaard N, Riehle MO, Wilkinson CD, Curtis AS (2004a) Investigating filopodia sensing using arrays of defined nano-pits down to 35 nm diameter in size. Int J Biochem Cell Biol **36**: 2005-2015.

Dalby MJ, Riehle MO, Johnstone H, Affrossman S, Curtis AS (2004b) Investigating the limits of filopodial sensing: A brief report using SEM to image the interaction between 10 nm high nano-topography and fibroblast filopodia. Cell Biol Int **28**: 229-236.

Dalby MJ, Gadegaard N, Tare R, Andar A, Riehle MO, Herzyk P, Wilkinson CD, Oreffo RO (2007) The control of human mesenchymal cell differentiation using nanoscale symmetry and disorder. Nat Mater **6**: 997-1003.

Dalby MJ, Gadegaard N, Wilkinson CD (2008) The response of fibroblasts to hexagonal nanotopography fabricated by electron beam lithography. J Biomed Mater Res A **84**: 973-979.

Engler AJ, Sen S, Sweeney HL, Discher DE (2006) Matrix elasticity directs stem cell lineage specification. Cell **126**: 677-689.

Fujita S, Ohshima M, Iwata H (2009) Time-lapse observation of cell alignment on nanogrooved patterns. J R Soc Interface **6 Suppl 3**: S269-277.

Garcia AJ, Boettiger D (1999) Integrin-fibronectin interactions at the cell-material interface: Initial integrin binding and signaling. Biomaterials **20**: 2427-2433.

Geiger B, Spatz JP, Bershadsky AD (2009) Environmental sensing through focal adhesions. Nat Rev **10**: 21-33.

Hamilton DW, Brunette DM (2007) The effect of substratum topography on osteoblast adhesion mediated signal transduction and phosphorylation. Biomaterials **28**: 1806-1819.

Hynes RO (2002) Integrins: Bidirectional, allosteric signaling machines. Cell **110**: 673-687.

Jeon H, Hidai H, Hwang DJ, Healy KE, Grigoropoulos CP (2010) The effect of micronscale anisotropic cross patterns on fibroblast migration. Biomaterials **31**: 4286-4295.

Juliano RL, Reddig P, Alahari S, Edin M, Howe A, Aplin A (2004) Integrin regulation of cell signalling and motility. Biochem Soc Tans **32**: 443-446.

Khatiwala CB, Peyton SR, Putnam AJ (2006) Intrinsic mechanical properties of the extracellular matrix affect the behavior of pre-osteoblastic Mc3t3-E1 cells. Am J Phys Cell Physiol **290**: C1640-C1650.

Kim DH, Han K, Gupta K, Kwon KW, Suh KY, Levchenko A (2009) Mechanosensitivity of fibroblast cell shape and movement to anisotropic substratum topography gradients. Biomaterials **30**: 5433-5444.

Kim JB, Leucht P, Luppen CA, Park YJ, Beggs HE, Damsky CH, Helms JA (2007) Reconciling the roles of FAK in osteoblast differentiation, osteoclast remodeling, and bone regeneration. Bone **41**: 39-51.

Lamers E, Walboomers FX, Domanski M, Te Riet J, Van Delft FC, Luttge R, Winnubst LA, Gardeniers HJ, Jansen JA (2010) The influence of nanoscale grooved substrates on osteoblast behavior and extracellular matrix deposition. Biomaterials **31**: 3307-3316.

Kirchner J, Kam Z, Tzur G, Bershadsky AD, Geiger B (2003) Live-cell monitoring of tyrosine phosphorylation in focal adhesions following microtubule disruption. J Cell Sci **116**: 975-986.

Lenhert S, Meier MB, Meyer U, Chi L, Wiesmann HP (2005) Osteoblast alignment, elongation and migration on grooved polystyrene surfaces patterned by Langmuir-Blodgett lithography. Biomaterials **26**: 563-570.

Liliensiek SJ, Wood JA, Yong JA, Auerbach R, Nealey PF, Murphy CJ (2010) Modulation of human vascular endothelial cell behaviors by nanotopographic cues. Biomaterials **31**: 5418-5426.

Loesberg WA, Te Riet J, Van Delft FC, Schon P, Figdor CG, Speller S, van Loon JJ, Walboomers XF, Jansen JA (2007) The threshold at which substrate nanogroove dimensions may influence fibroblast alignment and adhesion. Biomaterials **28**: 3944-3951.

Loesberg WA, Walboomers XF, Van Loon JJ, Jansen JA (2008) Simulated microgravity activates MAPK

pathways in fibroblasts cultured on microgrooved surface topography. Cell Mot Cytoskel **65**: 116-129.

Michiardi A, Aparicio C, Ratner BD, Planell JA, Gil J (2007) The influence of surface energy on competitive protein adsorption on oxidized niti surfaces. Biomaterials **28**: 586-594.

Owen GR, Meredith DO, ap Gwynn I, Richards RG (2005) Focal adhesion quantification – a new assay of material biocompatibility? Eur Cells Mater **9**: 85-96.

Pankov R, Endo Y, Even-Ram S, Araki M, Clark K, Cukierman E, Matsumoto K, Yamada KM (2005) A Rac switch regulates random versus directionally persistent cell migration. J Cell Biol **170**: 793-802.

Rosales-Leal JI, Rodriguez-Valverde MA, Mazzaglia G, Ramon-Torregrosa PJ, Diaz-Rodriguez L, Garcia-Martinez O, Vallecillo-Capilla M, Ruiz C, Cabrerizo-Vilchez MA (2010) Effect of roughness, wettability and morphology of engineered titanium surfaces on osteoblast-like cell adhesion. Colloids Surf A **365**: 222-229.

Shattil SJ, Kim C, Ginsberg MH (2010) The final steps of integrin activation: The end game. Nat Rev **11**: 288-300.

Steele JG, Johnson G, Underwood PA (1992) Role of serum vitronectin and fibronectin in adhesion of fibroblasts following seeding onto tissue culture polystyrene. J Biomed Mater Res **26**: 861-884.

Stone DA, Hsu L, Stupp SI (2009) Self-assembling quinquethiophene-oligopeptide hydrogelators. Soft Matter **5**: 1990-1993.

Su WT, Liao YF, Chu IM (2007) Observation of fibroblast motility on a micro-grooved hydrophobic elastomer substrate with different geometric characteristics. Micron **38**: 278-285.

Teixeira AI, Abrams GA, Bertics PJ, Murphy CJ, Nealey PF (2003) Epithelial contact guidance on well-defined micro- and nanostructured substrates. J Cell Sci **116**: 1881-1892.

Tocce EJ, Smirnov VK, Kibalov DS, Liliensiek SJ, Murphy CJ, Nealey PF (2010) The ability of corneal epithelial cells to recognize high aspect ratio nanostructures. Biomaterials **31**: 4064-4072.

Toworfe GK, Composto RJ, Adams CS, Shapiro IM, Ducheyne P (2004) Fibronectin adsorption on surface-activated poly(dimethylsiloxane) and its effect on cellular function. J Biomed Mater Res A **71A**: 449-461.

Tsai WB, Ting YC, Yang JY, Lai JY, Liu HL (2009) Fibronectin modulates the morphology of osteoblast-like cells (Mg-63) on nano-grooved substrates. J Mater Sci Mater Med **20**: 1367-1378

Uttayarat P, Chen M, Li M, Allen FD, Composto RJ, Lelkes PI (2008) Microtopography and flow modulate the direction of endothelial cell migration. Am J Phys **294**: H1027-1035.

Van Delft FCMJ, van den Heuvel FC, Loesberg WA, te Riet J, Schon P, Figdor CG, Speller S, van Loon JJWA, Walboomers XF, Jansen JA (2008) Manufacturing substrate nano-grooves for studying cell alignment and adhesion. Microel Eng **85**: 1362-1366.

Van Delft FCMJM, Weterings JP, van Langen-Suurling AK, Romijn H (2000) Hydrogen silsesquioxane/Novolak bilayer resist for high aspect ratio nanoscale electron-beam lithography. JVac Sci Technol B **18**: 3419-3423.

Walboomers XF, Croes HJ, Ginsel LA, Jansen JA (1998) Growth behavior of fibroblasts on microgrooved polystyrene. Biomaterials **19**: 1861-1868.

Walboomers XF, Jansen JA (2001) Cell and tissue behavior on micro-grooved surfaces. Odontology **89**: 2-11.

Weiner S, Wagner HD (1998) The material bone: Structure-mechanical function relations. Ann Rev Mater Sci **28**: 271-298.

Weiss P (1945) Experiments on cell and axon orientation in vitro - the role of colloidal exudates in tissue organization. J Exp Zool **100**: 353-386.

Wójciak-Stothard B, Madeja Z, Korohoda W, Curtis A, Wilkinson C (1995) Activation of macrophage-like cells by multiple grooved substrata. Topographical control of cell behaviour. Cell Biol Int **19**: 485-490

Wójciak-Stothard B, Curtis A, Monaghan W, MacDonald K, Wilkinson C (1996) Guidance and activation of murine macrophages by nanometric scale topography. **223**: 426-435

Wozniak MA, Modzelewska K, Kwong L, Keely PJ (2004) Focal adhesion regulation of cell behavior. Biochim Biophys Acta **1692**: 103-119.

Yang JY, Ting YC, Lai JY, Liu HL, Fang HW, Tsai WB (2008) Quantitative analysis of osteoblast-like cells (Mg63) morphology on nanogrooved substrata with various groove and ridge dimensions. J Biomed Mater Res A **90**: 629-640

Zaidel-Bar R, Itzkovitz S, Ma'ayan A, Iyengar R, Geiger B (2007) Functional atlas of the integrin adhesome. Nat Cell Bio **9**: 858-867.

Zhu B, Zhang Q, Lu Q, Xu Y, Yin J, Hu J, Wang Z (2004) Nanotopographical guidance of C6 glioma cell alignment and oriented growth. Biomaterials **25**: 4215-4223.

Discussion with Reviewers

Reviewer I: The manuscript advances works cited by the authors on the roles of nanoscale grooves and squares on cell adhesion, elongation, alignment and motility. Which of these substrates do the authors hypothesize would enhance osteospecific function in a clinical setting?

Authors: In the current study we observed different cellular response to various patterns. First, cell morphology is highly influenced by the use of different patterns (i.e. squares or grooves). Such differences in cell behavior can affect wound closure and tissue regeneration very differently. If cells are highly aligned to the grooves, this may possibly increase the organization of the newly formed bone matrix more distal from the implant. In a previous study, we already observed that mineralized matrix is specifically deposited inside the grooves in an aligned fashion by osteoblasts (Lamers *et al.*, 2010).

Second, cells cultured on patterns with wide grooves and small ridges (i.e., R:G 1:3) move rapidly, whereas cells on patterns with wide ridges are less motile. High cell

motility could possibly result in faster wound closure, as observed in guided tissue regeneration membranes (Behring *et al*., 2008). In contrast, Geiger *et al.* (2009, text reference) demonstrated that the inability of cells to form proper focal adhesions induced a high cell motility, but also cell death.

Therefore, several patterns are very interesting to study the bone regenerative process. Grooves with a R:G of 1:3 and a between of 300 nm would be interesting as they induce cells, become highly elongated and motile. In addition, grooves with a R:G of 1:1 and a pitch of 300 nm are interesting, since alignment and elongation is similar to the R:G of 1:3, however with significantly lower motility. Finally, squares with a spacing of 300 nm would also be very interesting, since these patterns induce a high motility, whereas morphology remains comparable to smooth substrates.

Currently, *in vivo* studies are performed to answer the question which of the substrates would enhance osteospecific function. Only such studies can answer which nanopatterns will exhibit clinical benefits when for instance applied to the surface of a dental or orthopedic implant

Reviewer I: Although parallel adhesion alignment is frequently observed on nano and microscale topographies. How do the authors explain the phenomenon of perpendicular focal adhesion formation commonly observed on these topographies?
Authors: The formation of focal adhesions is a highly dynamic process as cells are constantly interrogating the surface for adhesion points. Consequently, parallel but immature adhesions are being observed.

Moreover, as mentioned in the introduction, the minimal length of mature focal adhesions is approximately 2 μm. In several studies, it is observed that if ridges (or grooves) are sufficiently larger than 2 μm the alignment of cells and its focal adhesions, is decreasing (Den Braber *et al.*, 1999; Teixeira *et al.*, 2006). In addition, if groove widths are smaller than 75 nm, which is the minimal distance between two integrin pair in order to form mature focal adhesions, then mature FA can be formed over several ridges and even perpendicular to the grooves (Geiger *et al*., 2009, text reference). In this study we further observed that decreasing groove depths also induce a random focal adhesion orientation.

Reviewer II: One of the particular concerns with nanotopographies are that they will only affect cells in direct contact with the pattern. Can the authors comment on whether such surfaces would actually allow development of adequate multi-layered bone.
Authors: Our templating method should not be seen as a 3D scaffold allowing the regeneration of multiple layer tissues. The aim was to create an interface in which cells live in a symbiosis with the implant surface resulting in a decreased risk for implant failure. Here we envision such conditions can be achieved by mimicking the natural extracellular matrix of bone, which is in the nanometer scale.

We expect that osteoblast adhesion and the bone-formation will become more organized than in the currently used rough implants and that the risk for implant failure will thus be decreased.

Reviewer II: Secondarily, would such features work *in vivo* given the very small sizes?
Authors: Recently we implanted nanogrooved substrates subcutaneously and here we observed that cell behavior was highly influenced by such patterns down to at least a 150 nm pitch. This data is also currently prepared for submission. Further work will encompass bone implantation sites.

Additional References

Behring J, Junker R, Walboomers XF, Chessnut B, Jansen JA (2008) Toward guided tissue and bone regeneration: morphology, attachment, proliferation, and migration of cells cultured on collagen barrier membranes. A systematic review. Odontology **96**: 1-11.

Den Braber ET, de Ruijter JE, Ginsel LA, von Recum AF, Jansen JA (1998) Orientation of ECM protein deposition, fibroblast cytoskeleton, and attachment complex components on silicone microgrooved surfaces. J Biomed Mater Res **40**: 291-300.

Teixeira AI, McKie GA, Foley JD, Bertics PJ, Nealey PF, Murphy CJ (2006) The effect of environmental factors on the response of human corneal epithelial cells to nanoscale substrate topography. Biomaterials **27**: 3945-3954.